High-energy cryo x-ray nano-imaging at the ID16A beamline of ESRF

Julio Cesar da Silva, Alexandra Pacureanu, Yang Yang, Florin Fus, Maxime Hubert, Leonid Bloch, Murielle Salome, Sylvain Bohic, Peter Cloetens

PROCEEDINGS OF SPIE

SPIEDigitalLibrary.org/conference-proceedings-of-spie

High-energy cryo x-ray nano-imaging at the ID16A beamline of ESRF

Julio C. da Silva
Alexandra Pacureanu
Yang Yang
Florin Fus
Maxime Hubert
Leonid Bloch
Murielle Salome
Sylvain Bohic
Peter Cloetens

SPIE.

Invited Paper

High-energy cryo X-ray nanoimaging at the ID16A beamline of ESRF

Julio C. da Silva[a,*], Alexandra Pacureanu[a], Yang Yang[a], Florin Fus[a], Maxime Hubert[a], Leonid Bloch[a], Murielle Salome[a], Sylvain Bohic[a,b], and Peter Cloetens[a]

[a]ESRF - The European Synchrotron, 38000 Grenoble, France
[b]INSERM U836, (Team 6: Synchrotron Radiation and Medical Research), Grenoble Institute of Neuroscience, Grenoble 38000, France

ABSTRACT

The ID16A beamline at ESRF offers unique capabilities for X-ray nano-imaging, and currently produces the worlds brightest high energy diffraction-limited nanofocus. Such a nanoprobe was designed for quantitative characterization of the morphology and the elemental composition of specimens at both room and cryogenic temperatures. Billions of photons per second can be delivered in a diffraction-limited focus spot size down to 13 nm. Coherent X-ray imaging techniques, as magnified holographic-tomography and ptychographic-tomography, are implemented as well as X-ray fluorescence nanoscopy. We will show the latest developments in coherent and spectroscopic X-ray nanoimaging implemented at the ID16A beamline.

Keywords: nanoprobe, KB mirrors, nanoimaging, nanofocusing, synchrotron beamline, high-energy X-rays, coherent x-ray imaging, x-ray fluorescence imaging

1. INTRODUCTION

Nanoimaging refers to high-resolution imaging in which not only the pixel size of the image, but also the actual spatial resolution is in the nanometric scale. Nowadays the pixel size is almost fully customizable, but the spatial resolution of the image will depend on several factors such as the beam focus size in the case of X-ray fluorescence, which is a scanning technique, or in the case of magnified holography, where the focus size defines the point-spread-function of the system. Mechanical disturbances such as vibrations of the motors used to position and scan the sample, fluctuations of temperature and thermal drifts of the sample itself will tend to deteriorate the resolution of the image even if the spot size was small enough. The ID16A beamline was built to minimize those effects, by assuring the stability of the optics and of the sample, in order to obtain the smallest ever high-energy X-ray focal spot, which enables imaging at the nanometric scale.

The European Synchrotron (ESRF) has developed the ID16A station dedicated to nanoimaging within the phase I of its upgrade program. This was driven by the need to address new challenges arising from the varying range of spatial and temporal scales in the fields of energy, health, advanced materials, and the environment. The ID16A beamline is optimized for hard X-ray imaging and it is currently the longest beamline at the ESRF with a distance of $185\,m$ from the source to the sample position. It was designed to provide a high-degree of coherence for imaging, and stability for efficient nanofocusing using multilayer coated Kirkpatrick-Baez (KB) mirrors. The end-station is operated under vacuum (around $10^{-7}\,mbar$) at room temperature or at cryogenic temperature ($\sim 120\,Kelvins$). It uses a piezo-driven short-range hexapod stage, allowing accurate positioning and scanning of the sample under the control of capacitive sensors. The beamline can operate at two discrete energies: $17.05\,keV$ or $33.6\,keV$. The flux in the high energy configuration ranges from 6×10^9 to 4×10^{12} photons/s.

This new ID16A beamline targets quantitative 3D nanoscale characterization of the morphology and elemental composition of samples through the combination of imaging techniques that use coherent X-rays (holography[1,2]

*Correspondence to J.C.d.S.: E-mail: jdasilva@esrf.fr, Telephone: +33 (0)4 76 88 27 72

X-Ray Nanoimaging: Instruments and Methods III, edited by Barry Lai, Andrea Somogyi, Proc. of SPIE Vol. 10389, 103890F · © 2017 SPIE
CCC code: 0277-786X/17/$18 · doi: 10.1117/12.2275739

and ptychography[3–5]) and high-resolution X-ray fluorescence analysis (XRF).[6–8] This set of nanoimaging techniques can be used on a wide range of spatial scales, and there are multiple applications in life sciences, earth sciences, and materials engineering, which can lead to development of new nanotechnologies.

We present the developments in X-ray nanoimaging implemented at the ID16A beamline and important applications to materials and life sciences. We show how this new ID16A station can help to better exploit the nanoscale world by taking advantage of the high photon flux, high degree of X-ray coherence at high-energies, and the small focus size. Recently, ID16A has already succeeded in obtaining a focus size of $12 \times 12.6nm$ $(H \times V)$ at $33.6\,keV$ with a flux of up to 6×10^9 photons/s using specially designed KB mirrors,[9,10] which is currently the world's smallest focal spot at such a high energy.

2. THE NANOIMAGING TECHNIQUES AT THE ID16A BEAMLINE

In this section, we are going to briefly present the three main nanoimaging techniques available at the ID16A beamline of the ESRF: 1) magnified in-line X-ray holography, 2) X-ray fluorescence and 3) X-ray ptychography, both in the near– and far-field. While X-ray fluorescence takes advantage of the very small focal spot of the X-rays for the high-resolution elemental distribution imaging, in-line holography and ptychography benefit from the high degree of coherence of the X-rays delivered at the beamline. Figure 1 illustrates the application of those three techniques to a lithographic structure with the shape of a "Siemens Star" made of 200 nm thick gold, where the smallest elements measure only 50 nm. In addition, the combination of those techniques with tomography makes 3D imaging possible via holographic X-ray computed tomography (HXCT),[1,2] ptychographic X-ray computed tomography (PXCT)[11,12] or X-ray Florescence computed tomography (XRFCT).[6,8]

2.1 X-ray Fluorescence (XRF)

The ID16A beamline offers two major assets for XRF: the high-energy X-rays, which allows to excite relatively high-Z elements efficiently, and the small X-ray focal spot, which enables very high-resolution XRF imaging. XRF is a scanning microscopy technique in which a fluorescence spectrum for each spot is acquired. The characteristic emission of the element can therefore reveal the elemental composition of the sample within that spot. Since the focal spot at the sample position at ID16A end-station is only tens of nanometers in size, the scanning steps can be very small, which yields a very high-resolution XRF imaging. In order to minimize the possible self-absorption effects, and collect the maximum of the fluorescence signal, ID16A uses two fluorescence detectors, one at each side of the sample. These detectors are orthogonal to the incident beam. One of the major fields of applications of such a technique is in metallomics, in which XRF is used to identify the metals and other elements in cells. Recently, a work performed at ID16A used XRF to identify target sites in human ovarian carcinoma treated with organo-osmium complex, which exhibits anticancer activity. Figure 2 shows the XRF maps of a 500 nm-thick section of such cells treated for 24 h showing the elemental distribution of Os, Zn, P, and Ca, with $50\,nm$ step size.[13]

2.2 X-ray in-line holography

X-ray in-line holography is a coherent X-ray imaging technique which exploits the longitudinal diversity to retrieve the phase-contrast images, *i.e.*, holograms are acquired at different sample-to-detector distances in order to retrieve the phase.[1,2] Typically, 4 distances are used, because it allows to resolve the ambiguities of the contrast-transfer-function (CTF).[2] Using a focused beam and positioning the sample at defocused positions, one can obtain magnified holographic images and, consequently, higher resolution images.[1] In the latter, the focal spot works as point-spread-function and limits the resolution of the resulting image. Thus, one can benefit from the small X-ray focus at ID16A beamline to obtain high-resolution phase-contrast images of a sample using in-line holography. It is a full-field microscopy technique, which is faster than the scanning microscopy techniques, like XRF or ptychography. Its combination with tomography provides a multi-scale approach to 3D imaging and gives rise to HXCT. HXCT allows to obtain morphological and quantitative information in 3D by reconstructing the distribution of the electron density in the object. The correlative microscopy combining the XRF in 2D and 3D, and the phase imaging, makes it possible to supplement the information on the micro-structure with the chemical information of the sample.

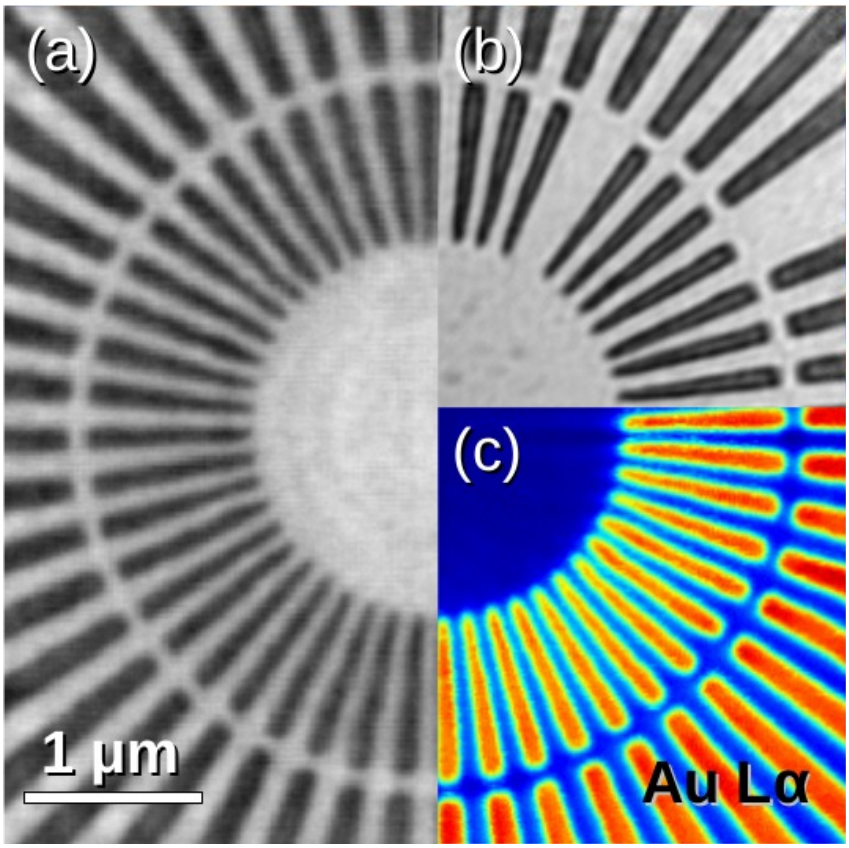

Figure 1. Illustration of the three techniques used at the ID16A nanoimaging beamline of the ESRF, applied to a lithographic structure with the shape of a "Siemens Star", made of 200 nm thick gold, in which the smallest features are only 50 nm in size. (a) In-line Holography. (b) X-ray Ptychography in the far field. (c) X-ray Fluorescence microscopy using the Au-Lα emission line, excited at 17.05 keV.

Recently, a study on titanium-vanadium-aluminum alloy (Ti-6Al-4V) was carried at ID16A by HXCT. An intensified intrinsic heat treatment was previously applied during selective laser melting of Ti-6Al-4V powder, using a scanning strategy that combines porosity-optimized processing with a very tight hatch distance. This enhances the resistance and the ductility needed for such an alloy to be used in the aerospace industry. Figure 3 shows the a volume obtained using HXCT, which provides sub-micron structural information on the alloy, which in turn assists with the characterization of such a material.[14]

2.3 Near- and far-field X-ray ptychography

Ptychography is a coherent X-ray imaging technique which simultaneously provides the absorption and phase-contrast images of the sample with potentially high-resolution and high sensitivity.[3,5,15–17] It yields as well the complex-valued illumination at the sample position, which can be directly used for wavefront sensing.[3,18] Ptychography at ID16A is implemented at high-energies (17.05 keV and 33.6 keV) with very high photon flux, which is quite unique and enables 2D and 3D imaging of highly absorbing and bulky samples with high-resolution. Such a scanning microscopy technique can be implemented in either near– and far-field regimes with some changes in the experimental setup and very few changes in the phase-retrieval algorithms.[4,19,20] It explores the redundancy of information given by the overlapping of different scanning spots and oversampling in the detector plane, for the ptychographic phase-retrieval procedure.[3,5] Both variations are available at ID16A nanoimaging beamline.

In the far-field regime, the beam is smaller than the sample and the scanning steps are chosen to overlap the different scanning spots. For each position, an interference pattern, related to the Fourier transform of

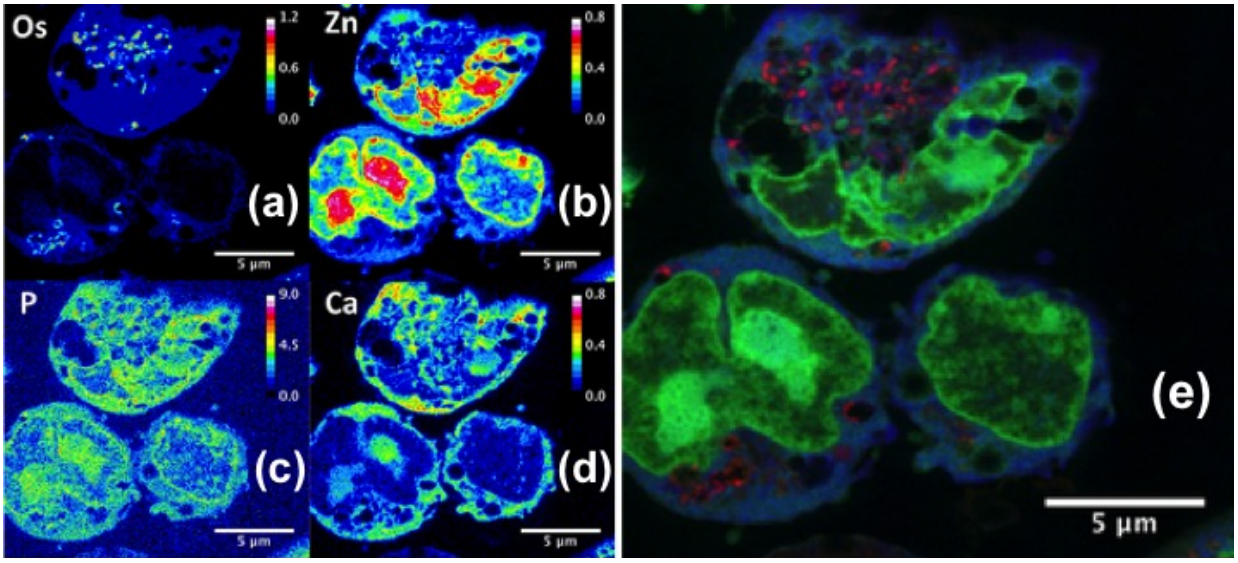

Figure 2. X-ray fluorescence maps of a 500 nm-thick section of human ovarian carcinoma cells treated for 24 h with organo-osmium complex. The cellular distribution of Os is shown in (a), of Zn in (b), of P in (c), and of Ca in (d). The calibration bar is in ng/mm^2. (e) Co-localization map of the elemental distribution of Os (red), Zn (green), and Ca (blue). The scan step size is $50\,nm$ with $50\,ms$ dwell time. Figure adapted from reference 13 previously published with Creative Commons license (CC BY 4.0).

the probed part of the sample, is recorded at the detector plane, located far downstream, in the Fraunhofer regime.[3,5,15] The resolution is independent of the focus size in this case. In the near-field regime, the sample is transversely translated within a coherent and structured beam, typically larger than the sample, inducing transverse diversity and redundancy needed for the phase retrieval.[20] For each position of the sample, an in-line hologram is recorded on the detector, in the holographic Fresnel regime. At the ID16A beamline, we record magnified holograms, thus we benefit from the small focal spot to obtain high resolution images. In both regimes, the images are reconstructed by iterative algorithms which try to reinforce the consistency between the different scanning positions and the acquired data for each of them, as well as the consistency among the different overlapping scanned regions.

Differently from other microscopy techniques which assume a homogeneous plane or spherical wave impinging onto the sample, ptychography has a big advantage because it can retrieve the illumination at the sample position, which is taken into account in the calculations. This allows avoiding artifacts in the reconstructed images which are caused by inhomogeneities in the incoming beam. In principle, the frequency mixture of the structured beams would even improve the quality of the reconstructed images as previously discussed.[3,20,21] Moreover, software tools are already available to the community for such reconstructions, and at the ID16A beamline we use the Python package Ptypy.[19] Finally, the combination of ptychography with tomography is part of the most recent developments on the beamline, and it can provide a 3D map of the complex-valued refractive index ($n(\vec{r}) = 1 - \delta(\vec{r}) + i\beta(\vec{r})$) of the sample with the highest spatial resolution that the beamline can offer. Thus, PXCT is fully quantitative[3] since we can obtain the electron density of a sample from the refractive index decrement, $\delta(\vec{r})$, and its linear attenuation coefficient from the absorption index, $\beta(\vec{r})$. At the ID16A beamline, PXCT has already been applied to many problems in life and material sciences.

3. CONCLUSIONS

We described here a nanoprobe at the ID16A beamline of the ESRF, which confines billions of high-energy X-ray photons per second in an a very small focal spot typically ranging from 13 to $30\,nm$. This nanoprobe will therefore allow better resolved imaging where the use of high energy X-rays is necessary and it is routinely available for scientific community. One can benefit from the high flux to be able to probe very small, localized

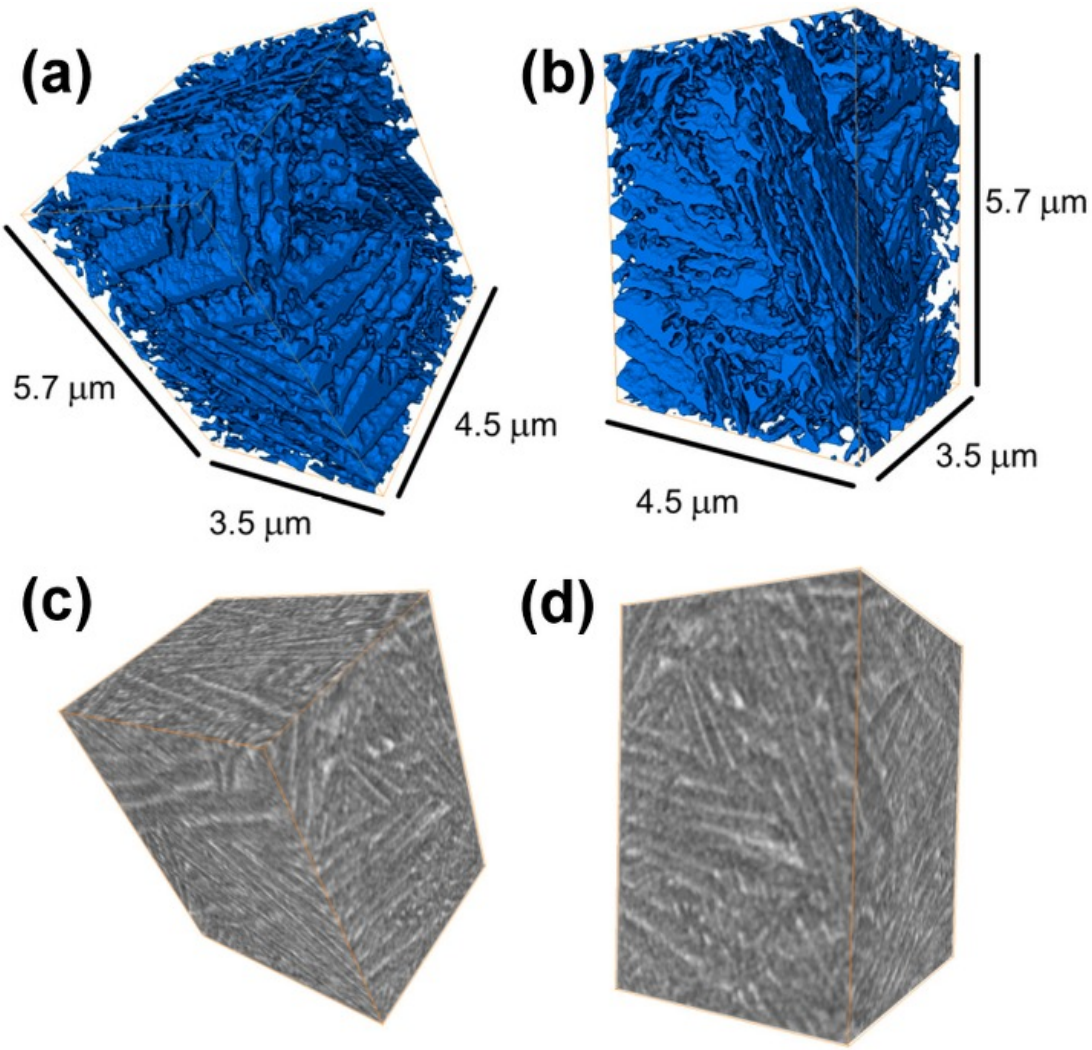

Figure 3. Tomographic volume of a Ti-6Al-4V alloy for applications in the aerospace industry retrieved by HXCT. (a,b) Rendering of different perspectives of the interconnected β network (in blue) segmented from corresponding (c,d) holographic X-ray computed tomography (HXCT) reconstruction (voxel size = $10\,nm^3$ and β matrix in bright grey) corresponding to a representative volume of the microstructure formed at the bottom part of the Ti-6Al-4V sample (*i.e.*, $z \approx 0\,mm$) upon selective laser melting (SLM). Figure adapted from reference 14 previously published with Creative Commons license (CC BY 4.0).

areas of the specimen with enough sensitivity in fluorescence and phase-contrast imaging experiments, which translate to high sensitivity to weak variations of electron density of a sample. Also, such a new nanoprobe can enable the imaging of highly-absorbing thick samples, commonly found in energy related materials or packaged semiconductor devices, or biological samples at cryogenic conditions with high resolution. Figure 1 showed that the high energy photons and small nanofocus allow the combination of coherent imaging with X-ray fluorescence analysis by exciting important high-Z elements like gold.

The achievements reached with the ID16A X-ray optics (KB mirrors) and optimized end-station represent significant advances in technology and applicability relative to previous developments, opening new routes in multidisciplinary fields. This is not only of significant interest to the broader X-ray optics and X-ray imaging community in synchrotrons, but it will also be appreciated by many research fields including life and material sciences.

ACKNOWLEDGMENTS

The authors acknowledge the technical support and instrumentation assistance of L. Andre, F. Villar, R. Baker, P. van der Linden, E. Gagliardini, Y. Dabin, A. Vivo, R. Barrett, C. Morawe, C. Jarnias, J. Morse, C. Cohen and O. Hignette. We also thank the assistance of S. Chalkidis, P. Thibault, and B. Enders with Ptypy.

REFERENCES

[1] Mokso, R., Cloetens, P., Maire, E., Ludwig, W., and Buffire, J.-Y., "Nanoscale zoom tomography with hard x rays using kirkpatrick-baez optics," *Appl. Phys. Lett.* **90**(14), 144104 (2007).

[2] Cloetens, P., Ludwig, W., Baruchel, J., Dyck, D. V., Landuyt, J. V., Guigay, J. P., and Schlenker, M., "Holotomography: Quantitative phase tomography with micrometer resolution using hard synchrotron radiation x rays," *Appl. Phys. Lett.* **75**(19), 2912–2914 (1999).

[3] da Silva, J. C. and Menzel, A., "Elementary signals in ptychography," *Opt. Express* **23**(26), 33812–33821 (2015).

[4] Thibault, P. and Menzel, A., "Reconstructing state mixtures from diffraction measurements," *Nature* **494**(7435), 68–71 (2013).

[5] Thibault, P., Dierolf, M., Menzel, A., Bunk, O., David, C., and Pfeiffer, F., "High-resolution scanning x-ray diffraction microscopy," *Science* **321**(5887), 379–382 (2008).

[6] Bleuet, P., Gergaud, P., Lemelle, L., Bleuet, P., Tucoulou, R., Cloetens, P., Susini, J., Delette, G., and Simionovici, A., "3d chemical imaging based on a third-generation synchrotron source," *Trends Analyt. Chem.* **29**(6), 518 – 527 (2010).

[7] Cauzid, J., Philippot, P., Bleuet, P., Simionovici, A., Somogyi, A., and Golosio, B., "3d imaging of vapour and liquid inclusions from the mole granite, australia, using helical fluorescence tomography," *Spectrochim. Acta Part B* **62**(8), 799 – 806 (2007).

[8] Golosio, B., Somogyi, A., Simionovici, A., Bleuet, P., Susini, J., and Lemelle, L., "Nondestructive three-dimensional elemental microanalysis by combined helical x-ray microtomographies," *Appl. Phys. Lett.* **84**(12), 2199–2201 (2004).

[9] da Silva, J. C., Pacureanu, A., Yang, Y., Bohic, S., Morawe, C., Barrett, R., and Cloetens, P., "Efficient concentration of high-energy x-rays for diffraction-limited imaging resolution," *Optica* **4**(5), 492–495 (2017).

[10] Morawe, C., Barrett, R., Cloetens, P., Lantelme, B., Peffen, J.-C., and Vivo, A., "Graded multilayers for figured kirkpatrick-baez mirrors on the new esrf end station id16a," *Proc. SPIE* **9588**, 958803–958803–7 (2015).

[11] Stockmar, M., Hubert, M., Dierolf, M., Enders, B., Clare, R., Allner, S., Fehringer, A., Zanette, I., Villanova, J., Laurencin, J., Cloetens, P., Pfeiffer, F., and Thibault, P., "X-ray nanotomography using near-field ptychography," *Opt. Express* **23**(10), 12720–12731 (2015).

[12] Dierolf, M., Menzel, A., Thibault, P., Schneider, P., Kewish, C. M., Wepf, R., Bunk, O., and Pfeiffer, F., "Ptychographic x-ray computed tomography at the nanoscale," *Nature* **467**(7314), 436–439 (2010).

[13] Sanchez-Cano, C., Romero-Caneln, I., Yang, Y., Hands-Portman, I. J., Bohic, S., Cloetens, P., and Sadler, P. J., "Synchrotron x-ray fluorescence nanoprobe reveals target sites for organo-osmium complex in human ovarian cancer cells," *Chem. Eur. J.* **23**(11), 2512–2516 (2017).

[14] Barriobero-Vila, P., Gussone, J., Haubrich, J., Sandlbes, S., Da Silva, J. C., Cloetens, P., Schell, N., and Requena, G., "Inducing stable + microstructures during selective laser melting of ti-6al-4v using intensified intrinsic heat treatments," *Materials* **10**(3), 268 (2017).

[15] Rodenburg, J. M., Hurst, A. C., Cullis, A. G., Dobson, B. R., Pfeiffer, F., Bunk, O., David, C., Jefimovs, K., and Johnson, I., "Hard-x-ray lensless imaging of extended objects," *Phys. Rev. Lett.* **98**, 034801 (2007).

[16] Faulkner, H. M. L. and Rodenburg, J. M., "Movable aperture lensless transmission microscopy: A novel phase retrieval algorithm," *Phys. Rev. Lett.* **93**, 023903 (2004).

[17] Hegerl, R. and Hoppe, W., "Dynamische theorie der kristallstrukturanalyse durch elektronenbeugung im inhomogenen primrstrahlwellenfeld," *Berichte der Bunsengesellschaft fr physikalische Chemie* **74**(11), 1148–1154 (1970).

[18] Thibault, P., Dierolf, M., Bunk, O., Menzel, A., and Pfeiffer, F., "Probe retrieval in ptychographic coherent diffractive imaging," *Ultramicroscopy* **109**(4), 338 – 343 (2009).

[19] Enders, B. and Thibault, P., "A computational framework for ptychographic reconstructions," *Proc. R. Soc. A* **472**(2196), 20160640 (2016).

[20] Stockmar, M., Cloetens, P., Zanette, I., Enders, B., Dierolf, M., Pfeiffer, F., and Thibault, P., "Near-field ptychography: phase retrieval for inline holography using a structured illumination," *Sci. Rep.* **3**, 1927 (2013).

[21] Guizar-Sicairos, M., Holler, M., Diaz, A., Vila-Comamala, J., Bunk, O., and Menzel, A., "Role of the illumination spatial-frequency spectrum for ptychography," *Phys. Rev. B* **86**, 100103 (2012).